

Timing of a Young Mildly Recycled Pulsar with a Massive White Dwarf Companion

P. Lazarus^{1*}, T. M. Tauris^{2,1}, B. Knispel^{3,4}, P. C. C. Freire¹,
J. S. Deneva⁵, V. M. Kaspi⁶, B. Allen^{3,4,7}, S. Bogdanov⁸,
S. Chatterjee⁹, I. H. Stairs¹⁰, and W. W. Zhu¹⁰

¹Max-Planck-Institut für Radioastronomie, Auf dem Hügel 69, 53121 Bonn, Germany

²Argelander-Institut für Astronomie, Universität Bonn, Auf dem Hügel 71, 53121 Bonn, Germany

³Max-Planck-Institut für Gravitationsphysik, D-30167 Hannover, Germany

⁴Leibniz Universität Hannover, D-30167 Hannover, Germany

⁵Naval Research Laboratory, 4555 Overlook Ave SW, Washington, DC 20375

⁶Dept. of Physics, McGill Univ., Montreal, QC H3A 2T8, Canada

⁷Physics Dept., U. of Wisconsin - Milwaukee, Milwaukee WI 53211, USA

⁸Columbia Astrophysics Laboratory, Columbia Univ., New York, NY 10027, USA

⁹Astronomy Dept., Cornell Univ., Ithaca, NY 14853, USA

¹⁰Dept. of Physics and Astronomy, Univ. of British Columbia, Vancouver, BC V6T 1Z1, Canada

11 September 2018

ABSTRACT

We report on timing observations of the recently discovered binary pulsar PSR J1952+2630 using the Arecibo Observatory. The mildly recycled 20.7-ms pulsar is in a 9.4-hr orbit with a massive, $M_{WD} > 0.93 M_{\odot}$, white dwarf (WD) companion. We present, for the first time, a phase-coherent timing solution, with precise spin, astrometric, and Keplerian orbital parameters. This shows that the characteristic age of PSR J1952+2630 is 77 Myr, younger by one order of magnitude than any other recycled pulsar–massive WD system. We derive an upper limit on the true age of the system of 150 Myr. We investigate the formation of PSR J1952+2630 using detailed modelling of the mass-transfer process from a naked helium star on to the neutron star following a common-envelope phase (Case BB Roche-lobe overflow). From our modelling of the progenitor system, we constrain the accretion efficiency of the neutron star, which suggests a value between 100 and 300% of the Eddington accretion limit. We present numerical models of the chemical structure of a possible oxygen–neon–magnesium WD companion. Furthermore, we calculate the past and the future spin evolution of PSR J1952+2630, until the system merges in about 3.4 Gyr due to gravitational wave emission. Although we detect no relativistic effects in our timing analysis we show that several such effects will become measurable with continued observations over the next 10 years; thus PSR J1952+2630 has potential as a testbed for gravitational theories.

Key words: pulsars: J1952+2630 – stars: neutron – white dwarfs – binaries: close – X-ray: binaries – stars: mass-loss

1 INTRODUCTION

Since 2004, the Arecibo L-band Feed Array (ALFA), a 7-beam receiver at the focus of the 305-m William E. Gordon radio telescope at the Arecibo Observatory, is being used to carry out the Pulsar–ALFA (PALFA) survey, a deep pulsar survey of low Galactic latitudes (Cordes et al.

2006; Lazarus 2013; Nice et al. 2013). Given its short pointings, the PALFA survey is especially sensitive to binary pulsars in tight orbits, as demonstrated by the discovery of the relativistic binary pulsar PSR J1906+0746, which did not require any acceleration search techniques (Lorimer et al. 2006). Another aspect of this and other modern Galactic plane surveys is the high time and frequency resolution, which allow the detection of millisecond pulsars (MSPs) at high dispersion measures (Champion et al. 2008; Deneva et al. 2012; Crawford et al. 2012) and there-

* E-mail: plazarus@mpifr-bonn.mpg.de

fore greatly expand the volume in which these can be discovered.

One of the innovative aspects of this survey is the use of distributed, volunteer computing. One of the main motivations is the detection of extremely tight (down to $P_b \sim 10$ minutes) binaries, for which acceleration and jerk searches become computationally challenging tasks. The analysis of survey data is distributed through the Einstein@Home (E@H) infrastructure (Knispel et al. 2010a; Allen et al. 2013). Thus far, the E@H pipeline has discovered 24 new pulsars in the PALFA survey data alone, complementing the other data analysis pipelines the PALFA survey employs (Quicklook, and PRESTO; Stovall et. al, in prep., and Lazarus et. al, in prep., respectively).

PSR J1952+2630 was the first binary pulsar discovered with the E@H pipeline (Knispel et al. 2011b). At that time the few observations available allowed only a rough estimate of the orbital parameters of this MSP based on Doppler measurements of the spin period. These already showed that PSR J1952+2630 has a massive WD companion ($M_{WD} > 0.945M_\odot$ assuming $M_p = 1.4M_\odot$), and may have evolved from an intermediate-mass X-ray binary (IMXB). Building on the analysis by Knispel et al. (2011b), we present in this paper the phase-coherent timing solution of PSR J1952+2630 resulting from dedicated follow-up observations with the Arecibo telescope, which provides orbital parameters far more precise than those previously determined. Our timing solution also shows the system is relatively young ($\tau_c = 77$ Myr).

It is commonly accepted that MSPs are spun up to their high spin frequencies via accretion of mass and angular momentum from a companion star (Alpar et al. 1982; Radhakrishnan & Srinivasan 1982; Bhattacharya & van den Heuvel 1991). In this recycling phase the system is observable as an X-ray binary (e.g. Hayakawa 1985; Nagase 1989; Bildsten et al. 1997) and towards the end of this phase as an X-ray MSP (Wijnands & van der Klis 1998; Papitto et al. 2013).

The majority of MSPs have helium WD companions and their formation is mainly channeled through low-mass X-ray binaries (LMXBs) which have been well investigated in previous studies (e.g. Webbink et al. 1983; Pylyser & Savonije 1988a, 1989b; Rappaport et al. 1995; Ergma et al. 1998; Tauris & Savonije 1999; Podsiadlowski et al. 2002; Nelson et al. 2004; van der Sluys et al. 2005). In contrast, binary pulsars, such as PSR J1952+2630, with relatively heavy WDs (CO or ONeMg WDs) are less common in nature. Their formation and recycling process involves a more massive WD progenitor star in an IMXB (see Tauris et al. 2011a, and references therein, for a discussion of their suggested formation channels). Here we distinguish IMXBs from other X-ray binaries as systems that leave behind a massive WD companion rather than a neutron star (NS). Some of these IMXB systems with donor stars of $6 - 7 M_\odot$ could also be classified observationally as Be/X-ray binaries since these stars are of spectral class B3-4 with emission lines. Recently, Tauris et al. (2012b) presented a detailed study of the recycling process of pulsars via both LMXBs and IMXBs and highlighted their similarities and differences. These authors also presented the first calculations of mild recycling in post common

envelope systems where mass transfer proceeds via so-called Case BB Roche-lobe overflow (RLO; see Sec. 4 for details).

PSR J1952+2630's combination of a young, massive WD in a close orbit with a recycled pulsar poses interesting questions about its formation and future evolution. Binary MSPs represent the advanced stage of stellar evolution in close, interacting binaries. Their observed orbital and stellar properties are thus fossil records of their evolutionary history. Therefore by using the precise description of a pulsar binary system determined from phase-coherent timing, and binary evolution modelling, we use PSR J1952+2630 as a probe of stellar astrophysics.

We also demonstrate that PSR J1952+2630 is an interesting test case for Case BB RLO, enabling interesting constraints on the accretion physics from the combined modelling of binary stellar evolution and the spin kinematics of this young, mildly recycled pulsar.

The rest of this paper is presented as follows: Sec. 2 describes the observations of PSR J1952+2630, and details of the data reduction and timing analysis. Results from this analysis are presented in Sec. 3. The binary evolution of the system is detailed in Sec. 4. The implications of our results, and future prospects are described in Secs. 5, and 6, respectively. Finally Sec. 7 summarizes the paper.

2 OBSERVATIONS AND DATA ANALYSIS

Following its discovery in 2010 July PSR J1952+2630 was observed during PALFA survey observing sessions using the usual survey observing set-up: the 7-beam ALFA receiver with the Mock spectrometers¹. In this set-up, ~ 322 MHz ALFA observing band was split into two overlapping sub-bands centred at 1300.1680 MHz and 1450.1680 MHz, each with a bandwidth of 172.0625 MHz. All timing observations using this set-up were performed with ALFA's central beam, and were typically 5-10 minutes in duration.

A dedicated timing program at the Arecibo Observatory started in 2011 November. The dedicated timing observations took data using the ‘‘L-wide’’ receiver. These data were divided into four non-overlapping, contiguous sub-bands recorded by the Mock spectrometers in search-mode. Each sub-band has 172 MHz of bandwidth divided in 2048 channels, sampled every $\sim 83.3 \mu\text{s}$. Together the four sub-bands cover slightly more than the maximum bandwidth of the receiver, 580 MHz, and are centred at 1444 MHz.

At the start of the dedicated timing campaign, three 3-hour observing sessions on consecutive days were conducted to obtain nearly complete orbital coverage, with the goal of detecting, or constraining a Shapiro delay signature caused by the pulsar's signal passing through its companions gravitational potential well.

Subsequently, monthly observations of 1 hour each were used for the next 11 months to monitor the pulsar, and refine our timing solution.

For analysis, each observation was divided into segments no longer than 15-minutes for each of the separate

¹ <http://www.naic.edu/~astro/mock.shtml>

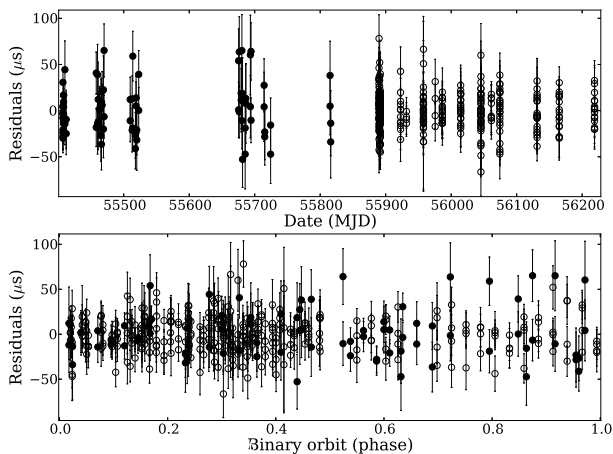


Figure 1. The difference between our pulsar TOAs and our timing solution. The filled circles are TOAs from data taken with the ALFA receiver, and the un-filled circles TOAs from data taken with the L-wide receiver. No systematic trends are visible as a function of epoch, or orbital phase.

sub-bands. Each segment was folded offline using the appropriate topocentric spin period using `prepfold` program from `PRESTO`². The resulting folded data files were converted to PSRFITS format (Hotan et al. 2004) with `pam` from the `psrchive` suite of pulsar analysis tools³. Data files were fully time and frequency integrated, and times-of-arrival (TOAs) were computed using `pat` from `psrchive`. The result was a single TOA for each ~ 15 minutes of observing for each sub-band.

TOAs for the different sub-bands were computed using a separate analytic template produced by fitting von Mises functions to the sum of profiles from the closely spaced three-day observing campaign. Profiles from different observations were aligned using the pulsar ephemeris.

Timing analysis was performed with the `TEMPO2` software (Hobbs et al. 2006). The phase-coherent timing solution determined fits the 418 pulse times-of-arrival. Our timing solution accurately models the timing data, leaving no systematic trends as a function of epoch, or orbital phase (see Fig. 1).

3 RESULTS

The timing analysis of PSR J1952+2630 has resulted in the determination of astrometric, spin, and Keplerian orbital parameters. The fitted timing parameters, as well as some derived parameters can be found in Table 1. The timing solution also includes a marginal detection of the proper motion of the pulsar.

3.1 The Nature of the Binary Companion Star

Given the combination of a relatively large observed mass function, $f = 0.153 M_{\odot}$ (see Table 1) and a small orbital eccentricity, $e = 4.1 \times 10^{-5}$, it is clear that PSR J1952+2630

has a massive WD companion. The minimum companion mass is $M_{\text{WD}}^{\text{min}} \approx 0.93 M_{\odot}$, obtained for an orbital inclination angle of $i = 90^{\circ}$ and an assumed NS mass, $M_{\text{NS}} = 1.35 M_{\odot}$. The small eccentricity excludes a NS companion star since the release of the gravitational binding energy alone, during the core collapse, would make the post-SN eccentricity much larger ($e \gg 0.01$; Bhattacharya & van den Heuvel 1991), in contrast with the observed value. Furthermore, no known double-neutron star system has $e < 0.01$, according to the ATNF Pulsar Catalogue⁴ (Manchester et al. 2005). Thus a double NS system is not possible and PSR J1952+2630 must have a massive WD companion, i.e. a carbon-oxygen (CO) or an oxygen-neon-magnesium (ONeMg) WD. The upper (Chandrasekhar) mass limit for a rigidly rotating WD is $\sim 1.48 M_{\odot}$ (e.g. Yoon & Langer 2005) and therefore we conclude that the WD companion star is in the mass interval $0.93 \lesssim M_{\text{WD}}/M_{\odot} \lesssim 1.48$.

The distance to PSR J1952+2630, estimated using the observed dispersion measure, and the NE2001 model of Galactic free electrons, is $d \simeq 9.6$ kpc (Cordes & Lazio 2002). The uncertainty in DM-derived distances using the NE2001 model can, in some cases, be up to a factor of ~ 2 off from the true distance. Unfortunately, this places the binary system too far away to hope to optically detect the WD companion with current telescopes. As expected, a search of optical and infrared catalogs yielded no counterpart.

3.2 The age of PSR J1952+2630

PSR J1952+2630 has a spin period of $P = 20.7$ ms and one of the highest values of the spin period derivative, $\dot{P} = 4.27 \times 10^{-18} \text{s s}^{-1}$ for any known recycled pulsar⁵ and by far the highest value for a mildly recycled pulsar with a massive WD companion. The observed value of \dot{P} is contaminated by kinematic effects (see Sec. 6). However, the contamination is only $\sim 0.01\%$, assuming our current value of the proper motion. The combination of P and \dot{P} of PSR J1952+2630 yields a small characteristic age, $\tau \equiv P/2\dot{P} \simeq 77$ Myr. The characteristic age of a pulsar should only be considered a rough order-of-magnitude estimate of the true age of the pulsar (i.e. time since recycling terminated). Thus the *true* ages are quite uncertain for recycled pulsars with large τ -values of several Gyr (Tauris 2012; Tauris et al. 2012b), unless a cooling age of their WD companion can be determined. However, the true ages of recycled pulsars with small values of τ (less than a few 100 Myr) are relatively close to the characteristic age. Hence, we conclude that PSR J1952+2630 is young, for a recycled pulsar, and in Secs 5.1 and 5.1.1 we discuss its true age (i.e. its actual age since it switched-on as a recycled radio pulsar) and also constrain its spin evolution in the past and in the future.

3.3 Constraints on the Binary System from Timing

Given the current timing data, the binary motion of PSR J1952+2630 can be accurately modelled without requiring any relativistic, post-Keplerian parameters. Unfor-

² <http://www.cv.nrao.edu/~sransom/presto/>

³ <http://psrchive.sourceforge.net/>

⁴ <http://www.atnf.csiro.au/people/pulsar/psrcat/>

⁵ This comparison was made using the ATNF Pulsar Catalogue.

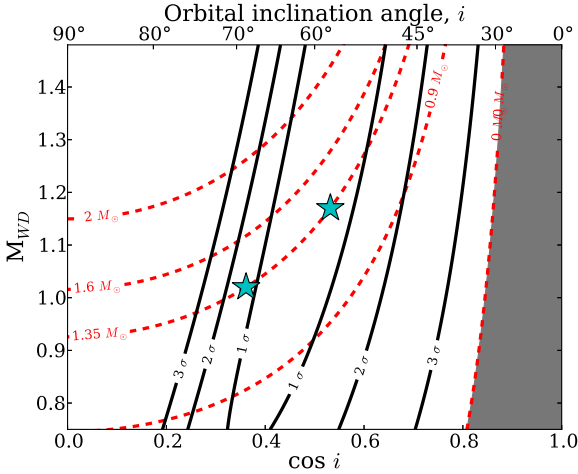


Figure 2. Map of companion-mass and inclination combinations allowed by the current timing data. The 1-, 2-, and 3- σ contours, shown in black, enclose ~ 68.3 , ~ 95.5 , and ~ 99.7 % of the allowed binary system configurations, respectively, given the current timing data, and requiring the companion’s mass to lie in the range $0.75 \leq M_{\text{WD}} \leq 1.48 M_{\odot}$. The red dashed lines trace constant pulsar mass. The grey region in the right is excluded because the pulsar mass must be larger than 0. The two stars are the results from the two simulations of the binary system’s evolution (see Sec. 4.1).

tunately, this means that the masses of the pulsar and its WD companion cannot be precisely determined by the current timing model.

Nevertheless, a χ^2 analysis was performed to investigate what constraints the lack of a Shapiro delay detection imposes on the make-up and geometry of the binary system (i.e. the mass of the pulsar, M_{NS} , and that of its companion, M_{WD} , as well as the binary system inclination, i , by using the mass-function). A χ^2 -map was computed using the `ChiSqCube` plug-in⁶ for `TEMPO2` (see Fig. 2). The χ^2 -map was computed for M_{WD} between 0 and $1.5 M_{\odot}$, in steps of $0.001 M_{\odot}$, and $\cos i$ from 0 to 1 in steps of 0.001.

For each point in the χ^2 -map the timing model was re-fit, holding the values of M_{WD} and $\cos i$ fixed. The resulting χ^2 values were converted to probabilities by following Splaver et al. (2002), and then normalized. The 1-, 2-, and 3- σ contours were chosen such that they contain ~ 68.3 , ~ 95.5 , and ~ 99.7 % of the allowed binary system configurations. Based on this analysis we know the binary system cannot be edge-on ($i = 90^\circ$). The inclination angle is constrained to be $i \leq 75^\circ$ for $M_{\text{NS}} \geq 1.35 M_{\odot}$, at the 3- σ level.

However, based on the massive companion, and small, but significantly non-zero eccentricity, we expect that with our current timing precision we will measure two (or possibly three) post-Keplerian parameters precisely enough to provide a stringent test of relativistic gravity, within the next 10 years (see Sec. 6).

⁶ The `ChiSqCube` plug-in populates a 3-dimensional χ^2 space. For the purpose of the analysis presented here, the third dimension was not used.

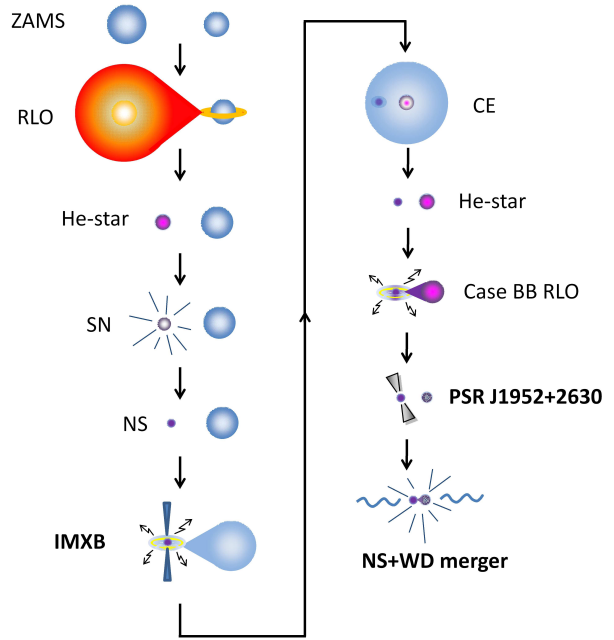


Figure 3. An illustration of the full binary stellar evolution from the zero-age main sequence (ZAMS) to the final merger stage. The initially more massive star evolves to initiate Roche-lobe overflow (RLO), leaving behind a naked helium core which collapses into a neutron star (NS) remnant, following a supernova explosion (SN). Thereafter, the system becomes a wide-orbit intermediate-mass X-ray binary (IMXB), leading to dynamically unstable mass transfer and the formation of a common envelope (CE), when the $6\text{--}7 M_{\odot}$ donor star initiates RLO. The post-CE evolution, calculated in detail in this paper, is responsible for recycling the NS via Case BB RLO when the helium star companion expands to initiate a final mass-transfer episode. PSR J1952+2630 is currently observed as a mildly recycled radio pulsar orbiting a massive white dwarf (WD). The system will merge in ~ 3.4 Gyr, possibly leading to a γ -ray burst-like event and the formation of a single black hole.

4 BINARY EVOLUTION OF THE PROGENITOR

In general, binary pulsars with a CO WD companion⁷ can form via different formation channels (see Tauris et al. 2012b, and references therein).

Pulsars with CO WDs in orbits of $P_{\text{orb}} \leq 2\text{--}3$ days, like PSR J1952+2630 ($P_{\text{orb}} = 9.4$ hr), are believed to have formed via a common envelope (CE) scenario. Such systems originate from IMXBs which have very large values of P_{orb} prior to the onset of the mass transfer. These systems are characterized by donor stars with masses between $2 < M_2/M_{\odot} < 7$, and very wide orbits up to $P_{\text{orb}} \simeq 10^3$ days. Donor stars near the tip of the red giant branch or on the asymptotic giant branch evolve via late Case B RLO or Case C RLO, respectively. As a result, these donor stars develop a deep convective envelope as they enter the giant phase, before filling their Roche lobe. These stars respond to mass loss by expanding, which causes them to overfill

⁷ Here, and in the following, we simply write ‘CO WD’ for any massive WD whose exact chemical composition (CO or ONeMg) is unknown.

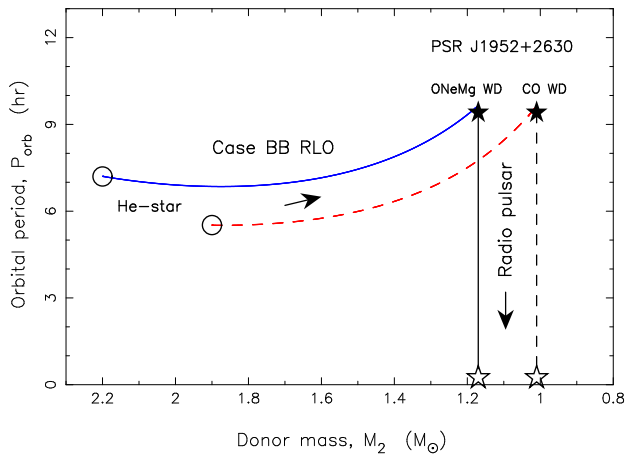


Figure 4. Progenitor evolution of the PSR J1952+2630 system in the (M_2, P_{orb}) -plane during mass transfer via Case BB RLO. The blue solid line is the evolutionary track for a $2.2 M_{\odot}$ helium star leaving a $1.17 M_{\odot}$ ONeMg WD remnant. The red dashed line is for a $1.9 M_{\odot}$ helium star leaving a $1.02 M_{\odot}$ CO WD remnant. The open circles show the location of the helium star donors at the onset of the RLO. The solid stars indicate the termination of the RLO when the radio pulsar turns on. In about 3.4 Gyr the system will merge (open stars).

their Roche lobe even more. Binaries where mass transfer occurs from a more massive donor star to a less massive accreting NS shrink in size, causing further overfilling of the donor star’s Roche lobe, which further enhances mass loss. This process leads to a dynamically unstable, runaway mass transfer and the formation of a CE (Paczynski 1976; Iben & Livio 1993; Ivanova et al. 2013). However, the wide orbit prior to the RLO is also the reason why these systems survive the CE and spiral-in phase, since the binding energy of donor star’s envelope becomes weaker with advanced stellar age, and therefore the envelope is easier to eject, thereby avoiding a merger event.

Given that the duration of the CE and spiral-in phase is quite short ($< 10^3$ yr; e.g. Podsiadlowski 2001; Passy et al. 2012; Ivanova et al. 2013) the NS can only accrete $\sim 10^{-5} M_{\odot}$ during this phase, assuming that its accretion is limited by the Eddington accretion rate (a few $10^{-8} M_{\odot} \text{ yr}^{-1}$). This small amount is not enough to even mildly recycle the pulsar. Instead, the NS is thought to be recycled during the subsequent so-called Case BB RLO (Tauris et al. 2012b). This post-CE mass-transfer phase is a result of the naked helium star (the stripped core of the original IMXB donor star) filling its Roche lobe when it expands to become a giant during helium shell burning. Hence, for the purpose of understanding the recycling of PSR J1952+2630 we only have to consider this epoch of evolution in detail. A complete overview of the full progenitor evolution of the system is illustrated in Fig. 3.

4.1 Calculations of Case BB RLO leading to Recycling of PSR J1952+2630

Binary evolution for NS–massive WD systems have been studied using detailed calculations of the Case BB RLO we

applied the Langer stellar evolution code (e.g. Tauris et al. 2011a, 2012b). However, none of the previously computed models produced systems sufficiently similar to that of PSR J1952+2630. We used the same code to study what progenitor systems can result in PSR J1952+2630-like binaries, the Case BB RLO of these systems, and the nature of the WD companion.

The masses of the WD and the NS (M_{WD} and M_{NS} , respectively) are not known from timing at this stage (see Sec. 3.3). In order to limit the number of trial computations, we assumed $M_{\text{NS}} = 1.35 M_{\odot}$ and performed various calculations with different values of initial orbital period and initial mass of the helium donor star, M_2 .

The young age of PSR J1952+2630 implies that P_{orb} (now 9.4 hours) has not changed much by gravitational wave radiation since the termination of the mass transfer (it was at most ~ 9.6 hours; see Sec. 5). Therefore we only select progenitor solutions of our modelling that have similar orbital periods. We also impose the criterion $M_{\text{WD}} = 0.93\text{--}1.48 M_{\odot}$, to be consistent with the minimum companion mass derived from our timing solution.

Two solutions satisfying our selection criteria are shown in Fig. 4. The first solution (blue solid line) is for a $2.2 M_{\odot}$ helium star leading to formation of a $1.17 M_{\odot}$ ONeMg WD. The second solution (red dashed line) is for a $1.9 M_{\odot}$ helium star leading to a $1.02 M_{\odot}$ CO WD. In both cases we assumed a helium star metallicity of $Z = 0.02$ (solar metallicity), a reasonable assumption given that their $\sim 6\text{--}7 M_{\odot}$ progenitors had short lifetimes of ~ 100 Myr and thus belong to Galactic Population I stars. The second solution predicts a shorter pulsar spin period at the termination of accretion, and therefore imposes a less strict limit on the mass-accretion efficiency; see Sec. 5.1 for a discussion.

Unfortunately, given the current timing data it is not possible to place sufficiently stringent constraints on the binary system to be used to select either of the two simulated scenarios as the actual evolution of the binary (see Sec. 3.3, and Fig. 2).

For the remainder of Sec. 4 we will consider only the ONeMg WD solution to our modelling. In particular, we will highlight some of the more interesting characteristics of the WD.

The mass-transfer rate, $|\dot{M}_2|$, for the solution leading to the $1.17 M_{\odot}$ ONeMg WD is shown in Fig. 5 as a function of time. The duration of the Case BB RLO is seen to last for about $\Delta t = 60$ kyr, which causes the NS to accrete an amount $\Delta M_{\text{NS}} \approx 0.7\text{--}6.4 \times 10^{-3} M_{\odot}$, depending on the assumed accretion efficiency and the exact value of the Eddington accretion limit, \dot{M}_{Edd} . Here we assumed $\dot{M}_{\text{Edd}} = 3.9 \times 10^{-8} M_{\odot} \text{ yr}^{-1}$ (a typical value for accretion of helium rich matter, Bhattacharya & van den Heuvel 1991) and allowed for the actual accretion rate to be somewhere in the interval 30–300% of this value. This is to account for the fact that the value of \dot{M}_{Edd} is derived under idealized assumptions of spherical symmetry, steady-state accretion, Thomson scattering opacity and Newtonian gravity. As we shall see, the accretion efficiency, and thus ΔM_{NS} , is important for the spin period obtained by the NS during its spin-up phase.

The mass-transfer rate from the helium star is highly super-Eddington ($|\dot{M}_2| \sim 10^3 \dot{M}_{\text{Edd}}$). The excess material (99.9%) is assumed to be ejected from the vicinity of the

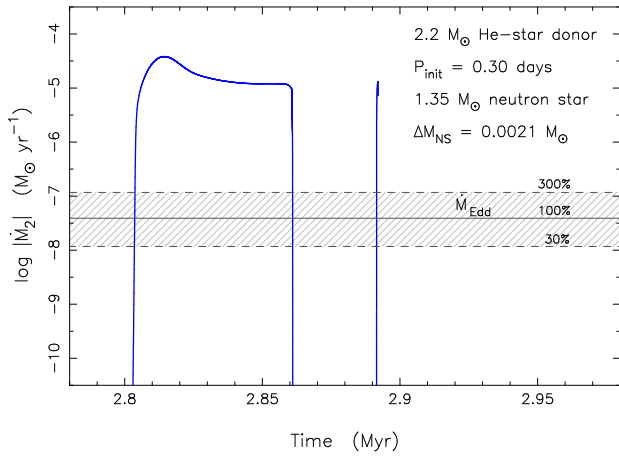


Figure 5. Mass-transfer rate as a function of stellar age for the progenitor evolution plotted in Fig. 4 leading to an ONeMg WD. The initial configuration is a $2.2 M_{\odot}$ helium star orbiting a $1.35 M_{\odot}$ NS with $P_{\text{orb}} = 0.30$ d. The Case BB RLO lasts for about 60 000 yr, then terminates for about 30 000 yr until a final vigorous helium shell flash is launched (the spike). The mass-transfer rate is seen to be highly super-Eddington ($\sim 10^3 \dot{M}_{\text{Edd}}$). The horizontal lines mark different values for the accretion efficiency in units of the Eddington accretion rate, \dot{M}_{Edd} . Depending on the exact value of \dot{M}_{Edd} , and the accretion efficiency, the NS accretes $0.7 - 6.4 \times 10^{-3} M_{\odot}$, which is sufficient to recycle PSR J1952+2630 – see text.

NS, in the form of a disc wind or a jet, with the specific orbital angular momentum of the NS following the so-called isotropic re-emission model (see Tauris et al. 2000c, and references therein).

4.2 Detailed WD structure

The calculated interior structure and evolution of a likely progenitor of PSR J1952+2630, a $2.2 M_{\odot}$ helium star which undergoes Case BB RLO and leaves behind an ONeMg WD, is illustrated in the “Kippenhahn diagram” (Kippenhahn & Weigert 1990) in Fig. 6. The plot shows the last 10 kyr of the mass-transfer phase ($t = 2.85\text{--}2.86$ Myr), followed by 32 kyr of evolution ($t = 2.860\text{--}2.892$ Myr) during which carbon is ignited in the detached donor star.

In our modelling of the companion star, there are four instances of off-centred carbon burning shells. These shells are the four blue regions underneath the green-hatched convection zones in Fig. 6. The ignition points are off-centre because these surrounding layers are hotter than the interior due to more efficient neutrino cooling in the higher-density inner core. The maximum temperature is near a mass coordinate of $m/M_{\odot} \simeq 0.4$.

The second carbon-burning shell penetrates to the centre of the proto-WD. However, at no point in the modelled evolution of the companion do the carbon burning shells, or the associated convection zones on top of these shells, reach the surface layers of the proto-WD. Therefore, the resulting WD structure is a hybrid, with a large ONeMg core engulfed by a thick CO mantle. The chemical abundance profile of the WD companion at the end of our modelling

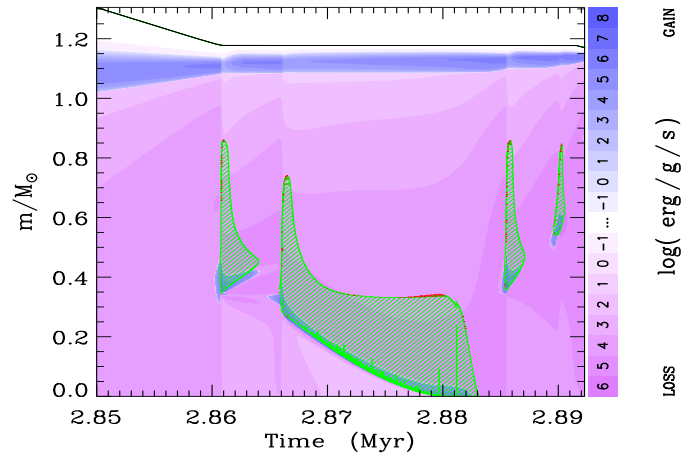


Figure 6. The Kippenhahn diagram showing the formation of an ONeMg WD companion to PSR J1952+2630. The plot shows cross-sections of the progenitor star in mass-coordinates from the centre to the surface, along the y-axis, as a function of stellar age (since the helium star ZAMS) on the x-axis. Only the last 42 kyr of our calculations are plotted. The Case BB RLO is terminated at time $t = 2.86$ Myr when the progenitor star has reduced its mass to $1.17 M_{\odot}$. The green hatched areas denote zones with convection. The intensity of the blue/purple colour indicates the net energy-production rate; the helium burning shell near the surface is clearly seen at $m/M_{\odot} \simeq 1.1$ as well the off-centred carbon ignition in shells, starting at $m/M_{\odot} \simeq 0.4$, defining the subsequent inner boundaries of the convection zones. The mixing of elements due to convection expands the ONeMg core out to a mass coordinate of about $m/M_{\odot} \simeq 0.85$ (see Fig. 7). Energy losses due to neutrino emission are quite dominant outside of the nuclear burning shells.

($t = 2.892$ Myr) is demonstrated in Fig. 7. Notice the tiny layer ($2.7 \times 10^{-2} M_{\odot}$) of helium at the surface which gives rise to a vigorous helium shell flash at $t = 2.892$ Myr. This shell flash can also be seen in Figs. 5 and 6 and gives rise to numerical problems for our code. We therefore end our calculations without resolving this flash. However, since the NS is only expected to accrete of the order $\sim 10^{-5} M_{\odot}$ as a result of this flash (based on modelling of similar binaries where we managed to calculate through such a helium shell flash), its impact on the final binary and spin parameters will be completely negligible.

As far as we are aware, this is the first presentation in the literature of detailed calculations leading to an ONeMg WD orbiting a recycled pulsar.

5 DISCUSSION

The future and past spin evolution of PSR J1952+2630 can be computed from the measured values of P and \dot{P} and assuming a (constant) braking index, n , which is defined by $\dot{\Omega} = -K\Omega^n$, where $\Omega = 2\pi/P$ and K is a scaling factor (Manchester & Taylor 1977). The resulting future and the past spin evolution of PSR J1952+2630 are shown in Fig. 8, top and bottom panel, respectively.

Given our modelling, the true age of PSR J1952+2630 is $\lesssim 150$ Myr. If a cooling age of the WD companion of a pulsar in a similar system could be accurately determined (for which the WD mass is needed), it would be possible to

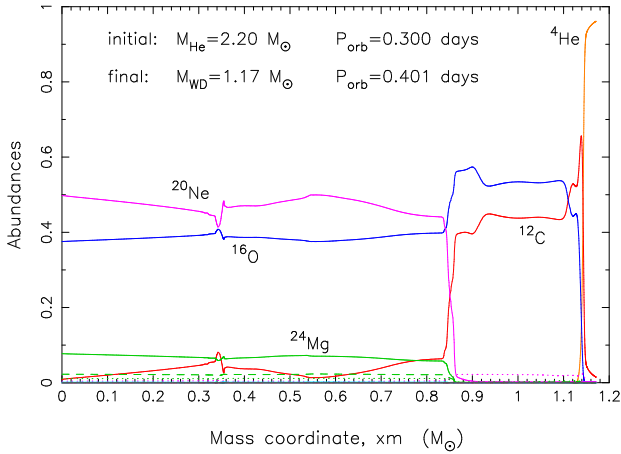


Figure 7. The chemical abundance structure of the ONeMg WD remnant (from our last calculated model at $t = 2.892$ Myr) of the Case BB RLO calculation shown in Figs. 4–6, one of the plausible solutions for PSR J1952+2630’s companion found in our modelling. This $1.17 M_{\odot}$ WD has a hybrid structure with an ONeMg core enclosed by a CO mantle and a tiny ($0.027 M_{\odot}$) surface layer of helium.

constrain the braking index of a recycled pulsar. Although this is not likely possible in the case of PSR J1952+2630 due to its large (DM) distance of 9.6 kpc, it may be feasible for other systems in the future.

The orbital decay due to gravitational wave radiation has also been computed (see Fig. 8, top). It is evident that P_{orb} has hardly decayed since the formation of PSR J1952+2630. Sec. 5.1 describes the implication for our binary stellar evolution modelling.

5.1 On the age and spin evolution of PSR J1952+2630

Our modelling of binary stellar evolution and accretion physics provides initial conditions for the spin of PSR J1952+2630, which must be consistent with current measurements. In particular, the spin period of PSR J1952+2630 predicted at the termination of accretion must be smaller than the observed spin period.

The minimum equilibrium spin period can be estimated given the amount of mass accreted by the NS, ΔM_{NS} . This quantity depends on our binary evolution models and the assumed accretion efficiency (in units of \dot{M}_{Edd} , see Fig. 5). Following Eqn. 14 of Tauris et al. (2012b),

$$P_{\text{ms}} = \frac{(M_{\text{NS}}/M_{\odot})^{1/4}}{(\Delta M_{\text{NS}}/0.22 M_{\odot})^{3/4}}, \quad (1)$$

where P_{ms} is the equilibrium spin period in units of ms, we estimate the minimum equilibrium spin period of PSR J1952+2630. These results are tabulated in Table 2, and compared with PSR J1952+2630’s current spin period in Fig. 8 (bottom). It is interesting to notice that we only obtain solutions for an accretion efficiency of 100% or 300%

of \dot{M}_{Edd} ⁸. If the accretion efficiency is smaller, the equilibrium spin period becomes larger than the present spin period of $P = 20.7$ ms, which is impossible.

The reason for the possibility of a lower initial spin period in case PSR J1952+2630 has a CO WD companion, is simply that the helium star progenitor of a CO WD has a lower mass and therefore evolves on a longer time-scale, thereby increasing ΔM_{NS} . Hence, a cooling age estimate of the WD companion could, in principle, also help constrain the accretion physics, because it puts limitations on the possible values of the initial spin period.

This is the first time an accretion efficiency has been constrained for a recycled pulsar which evolved via Case BB RLO. In contrast, the accretion efficiency of millisecond pulsars formed in low-mass X-ray binaries (LMXBs) has been shown to be much lower, about 30% in some cases (Tauris & Savonije 1999; Jacoby et al. 2005; Antoniadis et al. 2012). The reason for this difference in accretion efficiencies may be related to the extremely high mass-transfer rates during Case BB RLO which could influence the accretion flow geometry and thus \dot{M}_{Edd} . Furthermore, accretion disc instabilities (Lasota 2001; Coriat et al. 2012), which act to decrease the accretion efficiency in LMXBs, do not operate in Case BB RLO binaries, due to the high value of $|\dot{M}_2|$.

5.1.1 Evolution in the P - \dot{P} diagram

By integrating the pulsar spin deceleration equation: $\dot{\Omega} = -K\Omega^n$, assuming a constant braking index, n we obtain isochrones. The kinematic solution at time t (positive in the future, negative in the past) is given by:

$$P = P_0 \left[1 + (n-1) \frac{\dot{P}_0}{P_0} t \right]^{1/(n-1)} \quad (2)$$

$$\dot{P} = \dot{P}_0 \left(\frac{P}{P_0} \right)^{2-n}, \quad (3)$$

where $P_0 = 20.7$ ms and $\dot{P}_0 = 4.27 \times 10^{-18} \text{ss}^{-1}$ are approximately the present-day values of the spin period and its derivative. The past and future spin evolution of PSR J1952+2630 in the P - \dot{P} diagram are plotted in Fig. 9. The isochrones are calculated using Eqns. 2 and 3 where n varies from 2 to 5, for different fixed values of t in the future (rainbow colours) and past (brown). For each isochrone, the time is given by the well-known expression:

$$t = \frac{P}{(n-1)\dot{P}} \left[1 - \left(\frac{P_0}{P} \right)^{n-1} \right]. \quad (4)$$

These solutions, however, are purely based on rotational kinematics. As already discussed above, one must take the constraints obtained from binary evolution and accretion physics into account. Therefore, if the Case BB RLO is not able to spin up the pulsar to a value smaller than, for example, 15 ms, then the true age of PSR J1952+2630 cannot be much more than 40 Myr for all values of $2 \leq n \leq 5$. For

⁸ Solutions requiring larger-than- \dot{M}_{Edd} accretion efficiencies are in fact physically viable because assumptions made during the calculation of \dot{M}_{Edd} mean it is only a rough measure of the true limiting accretion rate.

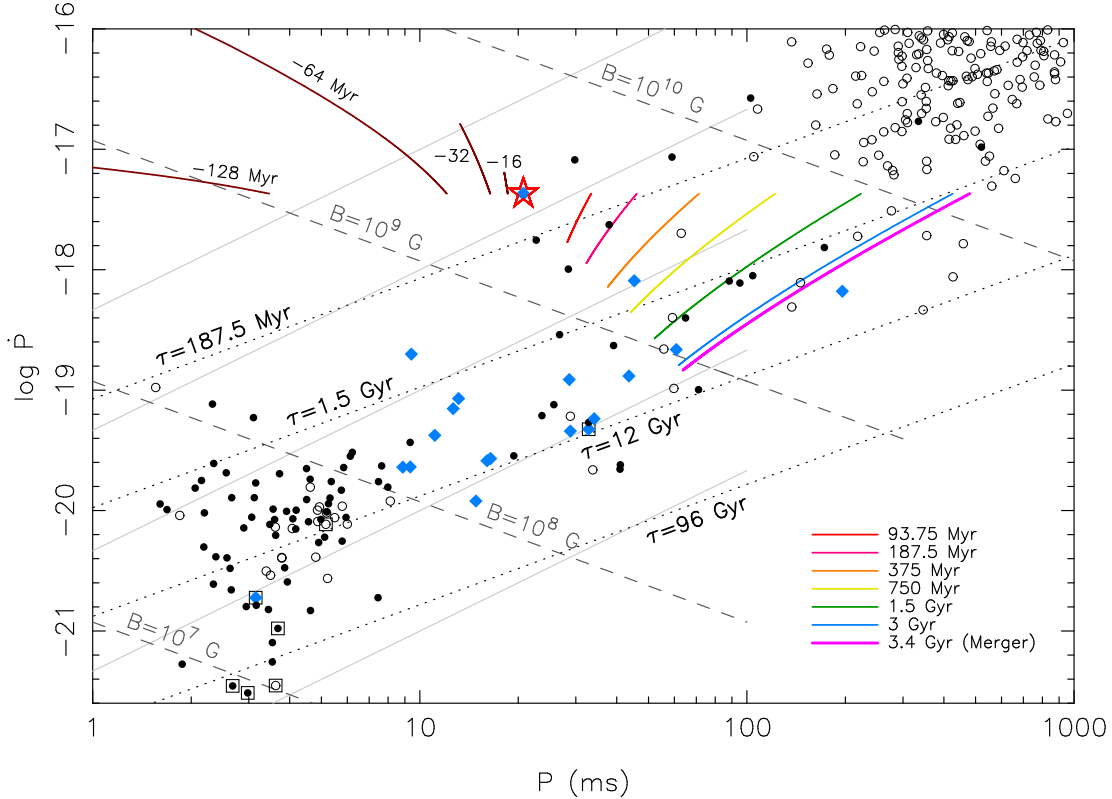


Figure 9. Isochrones of past (brown colour) and future evolution (rainbow colours) of PSR J1952+2630 in the P - \dot{P} diagram. The present location is marked by the open red star. All isochrones were calculated for braking indices in the interval $2 \leq n \leq 5$. Also plotted are inferred constant values of B -fields (dashed lines) and characteristic ages, τ (dotted lines). The thin grey lines are spin-up lines with $\dot{M}/\dot{M}_{\text{Edd}} = 1, 10^{-1}, 10^{-2}, 10^{-3}$ and 10^{-4} (top to bottom), assuming a pulsar mass of $1.4 M_{\odot}$. Observational data of the plotted Galactic field pulsars are taken from the ATNF Pulsar Catalogue in March 2013. Binary pulsars are marked with solid circles and isolated pulsars are marked with open circles. For further explanations of the calculations, and corrections to \dot{P} values see Tauris et al. (2012b). Binary pulsars with a massive (CO or ONeMg) WD companion are marked with a blue diamond. The past spin evolution of PSR J1952+2630 is particularly interesting as it constrains both the binary evolution and the recycling process leading to its formation – see text.

closer binary systems similar to PSR J1952+2630 where a cooling age determination of the WD is possible, such a measurement could be useful for constraining the birth period of the pulsar, as well as the system’s accretion efficiency.

Also shown in Fig. 9 is the future spin evolution of PSR J1952+2630 until the system merges in about 3.4 Gyr. It is interesting to notice that a system like PSR J1952+2630 should be observable as a radio pulsar binary until it merges, suggesting the existence of similar NS–massive WD binaries with much shorter orbital periods, to which PALFA is sensitive (Allen et al. 2013; Lazarus 2013). The unique location of PSR J1952+2630 with respect to other known recycled pulsars with a massive WD companion (marked with blue diamonds) is also clear from this figure. It is seen that only three other systems may share a past location in the P - \dot{P} diagram similar to that of PSR J1952+2630 (if $2 \leq n \leq 5$). This could suggest that such surviving post-CE systems are often formed with small values of P_{orb} which cause them to merge rapidly – either during the Case BB RLO or shortly thereafter due to gravitational wave radiation.

6 FUTURE PROSPECTS FOR PSR J1952+2630

We now investigate the future use of PSR J1952+2630 as a gravitational laboratory. Looking at Table 1, we can see that the eccentricity, e , and longitude of periastron, ω , can be measured quite precisely, in the latter case to within 1.2° , despite the small absolute value of the eccentricity, $4.1(1) \times 10^{-5}$. If we assume a mass of $1.35 M_{\odot}$ for the pulsar and $1.1 M_{\odot}$ for the WD, then general relativity predicts that ω should increase at a rate $\dot{\omega} = 1.72^{\circ} \text{yr}^{-1}$, which given the precision of ω implies that the effect should be detectable in the next few years. Measuring it will eventually give us an estimate of the total mass of the system (Weisberg & Taylor 1981).

Furthermore, thanks to PSR J1952+2630’s rather short orbital period, the shortest among recycled pulsar–massive WD systems, the rate of gravitational wave emission is much higher than for any other such system. This emission will cause the orbit to decay. For the same assumptions as above, the orbital period should change at a rate $\dot{P}_{\text{b,pred}} = -1.14 \times 10^{-13} \text{ s s}^{-1}$. As previously mentioned, this will cause the system to merge within about 3.4 Gyr.

The orbital decay due to the emission of gravitational waves is not measurable at present but it should be de-

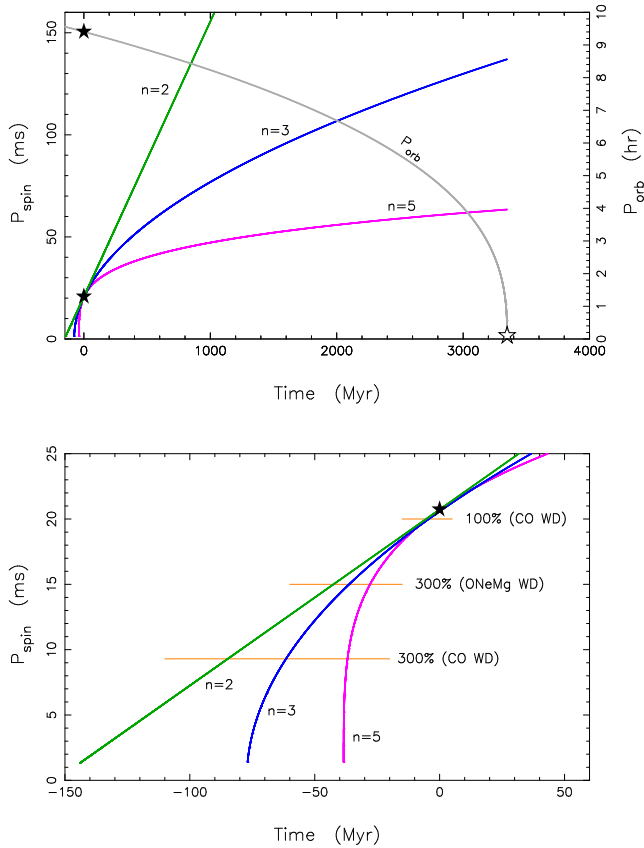


Figure 8. The future (top) and the past (bottom) spin evolution of PSR J1952+2630 for different values of the braking index, n . The location of PSR J1952+2630 at present is marked by a solid star. In the top panel, the grey curve shows the calculated orbital decay due to gravitational wave radiation until the system merges in about 3.4 Gyr (marked by an unfilled star). The lower panel is a zoom-in on the past spin evolution. Depending on n , the WD companion mass and the accretion efficiency of the NS during Case BB RLO, the pulsar could have been spun up to the initial spin periods indicated by the orange horizontal lines – see text for a discussion.

tectable in the near future. In order to verify this, we made simulations of future timing of this pulsar that assume similar timing precision as at present (a single 18- μ s TOA every 15 minutes for each of two 300-MHz bands centred around 1400 MHz). We assume two campaigns in 2015 and 2020, where the full orbit is sampled a total of 8 times, spread evenly for each of those years. The total observing time of 72 hours for each of those years is a realistic target. These simulations indicate that by the year 2020 \dot{P}_b should be detectable with 12- σ significance and $\dot{\omega}$ to about 9- σ significance.

The resulting constraints on the masses of the components and system inclination are depicted graphically in Fig. 10. We plot the 1- σ bands allowed by the ‘measurement’ of a particular parameter. The figure shows several interesting features. The first is that even with these measurements of \dot{P}_b and $\dot{\omega}$, it is not possible to determine the two masses accurately from them, given the way their 1- σ uncertainty bands intersect in the mass-mass diagram. The 1- σ band of h_3 (the orthometric amplitude of the Shapiro delay, see Freire & Wex 2010) intersects the others at a rather

sharp angle and can in principle be used to determine the masses more accurately. However, at the moment it is not clear whether h_3 is precisely measurable. A more massive companion in a less inclined orbit yields more pessimistic expectations, as depicted in Fig. 10.

Fortunately, very precise masses are not required to perform a test of general relativity using $\dot{\omega}$ and \dot{P}_b . As illustrated in Fig. 10, the bands allowed by $\dot{\omega}$ and \dot{P}_b are nearly parallel. As the precision of these measurements improves general relativity is tested by the requirement that the two bands still overlap. Fig. 10 also shows that even if we could determine h_3 precisely, the precision of this $\dot{\omega}$ - h_3 - \dot{P}_b test will be limited by the precision of the measurement of $\dot{\omega}$, because its uncertainty only decreases with $T^{-3/2}$ (where T is the timing baseline), while for \dot{P}_b the measurement uncertainty decreases with $T^{-5/2}$.

Eventually, though, the uncertainty of the measurement of $\dot{\omega}$ will become very small. At that stage the precision of this test will be limited by the precision of \dot{P}_b , which is limited by the lack of precise knowledge of the kinematic contributions (Damour & Taylor 1991):

$$\left(\frac{\dot{P}_b}{P_b}\right) = \left(\frac{\dot{P}_b}{P_b}\right)_{\text{obs}} - \frac{\mu^2 d}{c} - \frac{a(d)}{c}, \quad (5)$$

where the subscript ‘obs’ indicated the observed quantity, μ is the total proper motion, d is the distance to the pulsar and $a(d)$ is the (distance dependent) difference between the Galactic acceleration of the system and that of the Solar System Barycentre (SSB), projected along the direction from the SSB to the system. At present these cannot be estimated because the proper motion has not yet been measured precisely. However, they likely represent the ultimate constraint to the precision of this GR test, as in the case of PSR B1913+16 (Weisberg et al. 2010). For that reason, we now estimate the magnitude of these kinematic effects.

If we assume that the final proper motion is of the same order of magnitude as what is observed now ($\sim 6 \text{ mas yr}^{-1}$), then at the assumed DM-distance of 9.6 kpc the kinematic contribution to \dot{P}_b will be about $3 \times 10^{-14} \text{ s s}^{-1}$. This is four times smaller than $\dot{P}_{b,\text{pred}}$, as defined above, which means that if we can’t determine the distance accurately, then the real value for the intrinsic orbital decay, $\dot{P}_{b,\text{int}}$, cannot be measured with a relative precision better than about 25 %. Things improve if the proper motion turns out to be smaller.

Is such a measurement useful? The surprising answer is that it is likely to be so. For pulsar-WD systems, alternative theories of gravity, like Scalar-Tensor theories (see Damour & Esposito-Farèse 1998, and references therein) predict the emission of dipolar gravitational waves, which would result in an increased rate of orbital decay. In the case of PSR J1738+0333, the orbital decay for that system was measured only with a significance of 8- σ . However, the absolute difference between the \dot{P}_b predicted by GR and the observed value is so small that it introduces the most stringent constraints ever on these gravity theories (Freire et al. 2012). The implication is that for PSR J1952+2630, one should be able to derive similarly low limits. However, if the proper motion is significantly smaller, and/or if we are able to determine the distance independently, then this system can provide a much more stringent test of alternative theories of gravity. The main reason for this is that the limiting factor of the PSR J1738+0333 test is the lim-

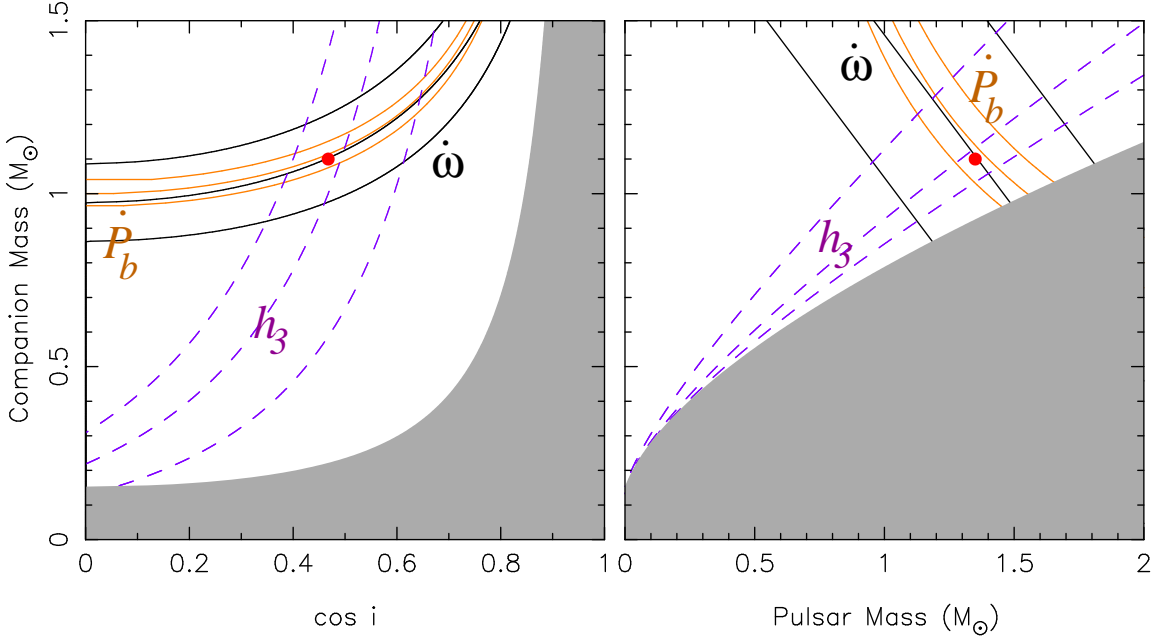


Figure 10. Constraints on system masses and orbital inclination from simulated radio timing of PSR J1952+2630. Each triplet of curves corresponds to the most likely value and standard deviations of the respective parameters; the region limited by it is the “1- σ ” band for that parameter. The masses and inclination used in the simulation are indicated by the red points. **Left:** $\cos i$ – M_{WD} plane. The grey region is excluded by the condition $M_{\text{NS}} > 0$. **Right:** M_{NS} – M_{WD} plane. The grey region is excluded by the condition $\sin i \leq 1$.

ited precision in the measurement of the component masses (Antoniadis et al. 2012) which would not be an issue for PSR J1952+2630, given the tighter constraints on the total mass that will eventually be derived from $\dot{\omega}$.

7 CONCLUSIONS

We have presented phase-coherent timing of PSR J1952+2630. Our timing model includes precise determinations of parameters describing the pulsar spin-down, astrometry and binary motion. No post-Keplerian orbital parameters are required. However, detailed modelling suggests the current pulsar–massive WD binary system evolved via post-CE Case BB RLO with an accretion efficiency which exceeded the Eddington limit by a factor of 1–3. We presented, for the first time, a detailed chemical abundance structure of an ONeMg WD orbiting a pulsar.

By projecting PSR J1952+2630’s orbital evolution into the future we estimate it will merge with its WD companion in ~ 3.4 Gyr due to the orbital decay from gravitational wave emission. Unfortunately, PSR J1952+2630 is too distant to make a detection of the cooling age of the pulsar’s WD companion. In the case of the discovery of a less distant analog of PSR J1952+2630 such a measurement could make it possible to constrain the braking index of the recycled pulsar, and/or the accretion efficiency during the Case BB RLO-phase. Also, timing observations over the next 10 years will result in the detection of the advance of periastron, and the orbital decay, enabling a test of general relativity. Finally, additional timing may also further elucidate the nature of the companion, and will permit

PSR J1952+2630 to be used to perform gravitational tests.

The Arecibo Observatory is operated by SRI International under a cooperative agreement with the National Science Foundation (AST-1100968), and in alliance with Ana G. Méndez-Universidad Metropolitana, and the Universities Space Research Association. Einstein@Home is supported by the Max Planck Society and US National Science Foundation (NSF) grants 1104902, 1104617, 1105572, and 1148523.

We thank Norbert Langer for discussions, as well as Jason Hessels and Aristeidis Noutsos for helpful comments.

PL acknowledges the support of IMPRS Bonn/Cologne and NSERC PGS-D. TMT gratefully acknowledges support and hospitality from the Argelander-Institut für Astronomie, Universität Bonn and the Max-Planck-Institut für Radioastronomie. BK acknowledges the support of the Max Planck Society. PCCF gratefully acknowledges financial support by the European Research Council for the ERC Consolidator Grant BEACON under contract no. 279702. BK acknowledges the support of the Max Planck Society. VMK was supported by an NSERC Discovery Grant, the Canadian Institute for Advanced Research, a Canada Research Chair, Fonds de Recherche Nature et Technologies, and the Lorne Trottier Chair in Astrophysics. Pulsar research at UBC is supported by an NSERC Discovery Grant and Discovery Accelerator Supplement.

REFERENCES

Allen B. et al., 2013, ApJ, 773, 91

- Alpar M. A., Cheng A. F., Ruderman M. A., Shaham J., 1982, *Nat.*, 300, 728
- Antoniadis J., van Kerkwijk M. H., Koester D., Freire P. C. C., Wex N., Tauris T. M., Kramer M., Bassa C. G., 2012, *MNRAS*, 423, 3316
- Bhattacharya D., van den Heuvel E. P. J., 1991, *Phys. Rep.*, 203, 1
- Bildsten L. et al., 1997, *ApJ Supp.*, 113, 367
- Champion D. J. et al., 2008, *Science*, 320, 1309
- Cordes J. M., Lazio T. J. W., 2002, arXiv:astro-ph/0207156
- Cordes J. M. et al., 2006, *ApJ*, 637, 446
- Coriat M., Fender R. P., Dubus G., 2012, *MNRAS*, 424, 1991
- Crawford F. et al., 2012, *ApJ*, 757, 90
- Damour T., Esposito-Farèse G., 1998, *Phys. Rev. D*, 58, 042001
- Damour T., Taylor J. H., 1991, *ApJ*, 366, 501
- Deneva J. S. et al., 2012, *ApJ*, 757, 89
- Ergma E., Sarna M. J., Antipova J., 1998, *MNRAS*, 300, 352
- Freire P. C. C., Wex N., 2010, *MNRAS*, 409, 199
- Freire P. C. C. et al., 2012, *MNRAS*, 423, 3328
- Hayakawa S., 1985, *Phys. Rep.*, 121, 317
- Hobbs G. B., Edwards R. T., Manchester R. N., 2006, *MNRAS*, 369, 655
- Hotan A. W., van Straten W., Manchester R. N., 2004, *PASA*, 21, 302
- Iben Jr. I., Livio M., 1993, *PASP*, 105, 1373
- Ivanova N. et al., 2013, *A&A Rev.*, 21, 59
- Jacoby B. A., Hotan A., Bailes M., Ord S., Kulkarni S. R., 2005, *ApJL*, 629, L113
- Kippenhahn R., Weigert A., 1990, *Stellar Structure and Evolution*. Springer, Berlin
- Knispel B. et al., 2010a, *Science*, 329, 1305
- Knispel B. et al., 2011b, *ApJL*, 732, L1
- Lasota J.-P., 2001, *New Astron. Rev.*, 45, 449
- Lazarus P., 2013, in *IAU Symposium*. pp 35–40
- Lorimer D. R. et al., 2006, *ApJ*, 640, 428
- Manchester R. N., Taylor J. H., 1977, *Pulsars*. W. H. Freeman, San Francisco
- Manchester R. N., Hobbs G. B., Teoh A., Hobbs M., 2005, *AJ*, 129, 1993
- Nagase F., 1989, *PASJ*, 41, 1
- Nelson L. A., Dubeau E., MacCannell K. A., 2004, *ApJ*, 616, 1124
- Nice D. J. et al., 2013, *ApJ*, 772, 50
- Paczýński B., 1976, in P. Eggleton, S. Mitton, & J. Whelan ed., *IAU Symposium Vol. 73, Structure and Evolution of Close Binary Systems*. Dordrecht, Holland, pp 75–+
- Papitto A. et al., 2013, *Nat.*, 501, 517
- Passy J.-C. et al., 2012, *ApJ*, 744, 52
- Podsiadlowski P., 2001, in P. Podsiadlowski, S. Rappaport, A. R. King, F. D’Antona, & L. Burderi ed., *Astronomical Society of the Pacific Conference Series Vol. 229, Evolution of Binary and Multiple Star Systems*. pp 239–+
- Podsiadlowski P., Rappaport S., Pfahl E. D., 2002, *ApJ*, 565, 1107
- Pylyser E., Savonije G. J., 1988a, *A&A*, 191, 57
- Pylyser E. H. P., Savonije G. J., 1989b, *A&A*, 208, 52
- Radhakrishnan V., Srinivasan G., 1982, *Current Science*, 51, 1096
- Rappaport S., Podsiadlowski P., Joss P. C., Di Stefano R., Han Z., 1995, *MNRAS*, 273, 731
- Splaver E. M., Nice D. J., Arzoumanian Z., Camilo F., Lyne A. G., Stairs I. H., 2002, *ApJ*, 581, 509
- Tauris T. M., 2012, *Science*, 335, 561
- Tauris T. M., Savonije G. J., 1999, *A&A*, 350, 928
- Tauris T. M., van den Heuvel E. P. J., Savonije G. J., 2000c, *ApJL*, 530, L93
- Tauris T. M., Langer N., Kramer M., 2011a, *MNRAS*, 416, 2130
- Tauris T. M., Langer N., Kramer M., 2012b, *MNRAS*, 425, 1601
- Webbink R. F., Rappaport S., Savonije G. J., 1983, *ApJ*, 270, 678
- Weisberg J. M., Taylor J. H., 1981, *General Relativity and Gravitation*, 13, 1
- Weisberg J. M., Nice D. J., Taylor J. H., 2010, *ApJ*, 722, 1030
- Wijnands R., van der Klis M., 1998, *Nat.*, 394, 344
- Yoon S.-C., Langer N., 2005, *A&A*, 435, 967
- van der Sluys M. V., Verbunt F., Pols O. R., 2005, *A&A*, 431, 647

Table 1. Fitted and derived parameters for PSR J1952+2630.

Parameter	Value ^a
<i>General Information</i>	
MJD Range	55407 – 56219
Number of TOAs	418
Weighted RMS of Timing Residuals (μs)	19
Reduced- χ^2 value ^b	1.03
MJD of Period Determination	55813
Binary Model Used	ELL1
<i>Fitted Parameters</i>	
R.A., α (J2000)	19:52:36.8401(1)
Dec., δ (J2000)	26:30:28.073(2)
Proper motion in R.A., μ_α (mas/yr)	-6(2)
Proper motion in Dec., μ_δ (mas/yr)	0(3)
Spin Frequency, ν (Hz)	48.233774295845(7)
Spin Frequency derivative, $\dot{\nu}$ ($\times 10^{-15}$ Hz/s)	-9.9390(5)
Dispersion Measure, DM (pc cm^{-3})	315.338(2)
Projected Semi-Major Axis, $a \sin i$ (lt-s)	2.798196(2)
Orbital Period, P_b (days)	0.39187863896(7)
Time of Ascending Node, T_{asc} (MJD)	55812.89716459(4)
ϵ_1	-0.000038(1)
ϵ_2	0.000015(1)
<i>Derived Parameters</i>	
Spin Period, (ms)	20.732360562672(3)
Spin Period Derivative ($\times 10^{-18} \text{s s}^{-1}$)	4.2721(2)
Galactic longitude, l ($^\circ$)	63.254
Galactic latitude, b ($^\circ$)	-0.376
Distance (NE2001, kpc)	9.6
Orbital Eccentricity, e ($\times 10^{-5}$)	4.1(1)
Longitude of Periastron, ω ($^\circ$)	291(2)
Mass Function, f (M_\odot)	0.153184(1)
Characteristic Age, $\tau_c = P/(2\dot{P})$ (Myr)	77
Inferred Surface Magnetic Field Strength, B_S ($\times 10^9$ G)	9.5
Spin-down Luminosity, \dot{E} ($\times 10^{35}$ ergs/s)	0.19

^aThe numbers in parentheses are the 1- σ , TEMP02-reported uncertainties on the last digit.

^bThe uncertainties of the ALFA and L-wide data sets were individually scaled such that the reduced χ^2 of the data sets are 1.

Table 2. Equilibrium spin obtained via Case BB RLO.

Acc. eff.	Δt_{RLO} (kyr)	ΔM_{NS} (M_\odot)	P (ms)
<i>2.2 M_\odot He star \rightarrow 1.17 M_\odot ONeMg WD</i>			
30%	57	0.7×10^{-3}	80
100%	61	2.1×10^{-3}	35
300%	61	6.4×10^{-3}	15
<i>1.9 M_\odot He star \rightarrow 1.02 M_\odot CO WD</i>			
30%	113	1.5×10^{-3}	45
100%	119	4.4×10^{-3}	20
300%	113	12.4×10^{-3}	9.3